

Wuling San Based on Network Pharmacology and *in vivo* Evidence Against Hyperuricemia via Improving Oxidative Stress and Inhibiting Inflammation

Jing Huang, Zhijian Lin , Yu Wang, Xueli Ding, Bing Zhang 

School of Chinese Materia Medica, Beijing University of Chinese Medicine, Beijing, People's Republic of China

Correspondence: Bing Zhang, School of Chinese Materia Medica, Beijing University of Chinese Medicine, Beijing, People's Republic of China, Email zhangb@bucm.edu.cn

Background: Hyperuricemia (HUA) is a major public health issue with a high prevalence worldwide. Wuling San (WLS) is an effective treatment for HUA. However, the active compounds and the related mechanism are unclear. In this study, we aimed to explore the active compounds and the underlying pharmacological mechanisms of WLS against HUA.

Methods: First, a network pharmacology approach was used to detect active compounds of WLS, and potential targets and signaling pathways involved in the treatment of HUA were predicted. Then, a molecular docking strategy was used to predict the affinity between active compounds and key targets. Finally, to verify the prediction, the HUA rat model was established.

Results: 49 active compounds with 108 common targets were obtained. Besides, cerevisterol, luteolin, ergosterol peroxide, beta-sitosterol, and sitosterol were identified as key active compounds. In PPI analysis, TNF, IL6, CASP3, PPARG, STAT3, and other 12 core targets were obtained. GO enrichment analysis indicated that WLS was likely to interfere with oxidative stress in the treatment of HUA, and KEGG enrichment analysis indicated multiple inflammation-related signaling pathways possibly involved in the treatment of HUA by WLS, including TNF, and NOD-like receptor, HIF-1, PI3K-Akt, and IL-17 signaling pathways. The results of molecular docking indicated that the active compounds had good binding properties to their key targets. In the validation experiments, WLS significantly reduced the levels of serum uric acid (SUA) and serum malondialdehyde (MDA). Moreover, WLS not only significantly increased the levels of total antioxidant capacity (T-AOC) and superoxide dismutase (SOD), but also inhibited the expression of tumor necrosis factor- α (TNF- α) and interleukin-6 (IL-6).

Conclusion: In the present study, we demonstrate that WLS has multicomponent, multitarget, and multi-pathway properties in the treatment of HUA. Its potential capability to reduce SUA could be ascribed to oxidative stress improvement and inflammation inhibition.

Keywords: hyperuricemia, Wuling San, oxidative stress, inflammation

Introduction

Hyperuricemia (HUA) is a common metabolic disorder characterized by an abnormally high level of SUA. It results from a reduction in UA excretion or an increase in UA production, or both. In mainland China, the prevalence of HUA in the general population was 17.4% (22.7% in males and 11.0% in females),¹ which became a major public health concern.

In addition to the well-known association with gout, increased SUA has been reported to play a critical role in cardiometabolic diseases, including hypertension,² atrial fibrillation,³ chronic kidney disease,⁴ type 2 diabetes,⁵ obesity,⁶ hypertriglyceridemia,⁷ metabolic syndrome⁸ and non-alcoholic fatty liver disease.⁹

Increased UA levels reflect an increase in xanthine oxidase (XO) enzymatic activity, which also results in an increased production of reactive oxygen species (ROS), leading to oxidative stress.¹⁰ Oxidative stress can activate several transcription factors, resulting in differential expression of certain genes involved in inflammation. Furthermore, inflammation caused by oxidative stress is the cause of many chronic diseases.¹¹ Inflammation and oxidative stress are implicated in the mechanisms underlying HUA-mediated chronic kidney injury,¹² and cardiovascular diseases.^{13–15}

Uric acid-lowering therapy (ULT) is widely used to treat HUA and prevent gout. The 2020 American College of Rheumatology (ACR) guidelines recommended that the target level of SUA in patients with ULT should be less than 6 mg/dl.¹⁶ At present, the anti-HUA drugs in clinical practice include allopurinol, febuxostat, probenecid, and benz-bromarone. However, anti-HUA reagents often cause adverse effects such as allopurinol hypersensitivity reactions,¹⁷ toxic epidermal necrolysis,¹⁸ abnormal liver and kidney function tests,¹⁹ blood dyscrasias, and urolithiasis.²⁰ There is growing evidence that natural medicines play a significant role in lowering UA.^{21–24} Therefore, exploring natural and nontoxic anti-HUA drugs from traditional Chinese medicine or natural compounds has become a research hotspot.

WLS (also called Oryeongsan in Korea and Gore-san or TJ-17 in Japan), recognized as a safe medicine since ancient times, originally recorded in the ancient traditional Chinese medicine book “Treatise on Febrile Diseases” (Shanghan Lun or Shanghan Zabing Lun in Chinese), written by Zhang Zhongjing in the third century.²⁵ WLS is a well-known and widely prescribed blend of traditional Chinese herbal medicine that consists of *Polyporus*, *Poria*, *Alismatis Rhizoma*, *Atractylodis Macrocephalae Rhizoma*, *Cinnamomi Ramulus*. In the Pharmacopoeia of the People’s Republic of China (2010 edition), it is recorded as effective for warming the Yang, promoting Qi transformation, and relieving dampness, diuresis and detumescence. It has been shown that WLS protects against kidney dysfunction in high fructose-induced HUA mice by enhancing urate excretion and improving kidney function.^{26,27} Meanwhile, WLS exerts extremely potent anti-inflammatory effects in LPS-stimulated macrophages.²⁸

WLS has been used as a therapeutic agent to treat a wide variety of diseases for thousands of years. Although studies have explored the role of WLS in HUA, its underlying molecular mechanisms and active substances were not specifically sought. Network pharmacology is a growing discipline that involves the study of constructing multi-layered networks of disease phenotypes, genes, and drugs. In contrast to the traditional “one disease-one target-one drug” paradigm, network pharmacology explores the interaction between the body and drug by mapping drug-target-disease networks at a biological level.²⁹ It emphasizes the paradigm shift from “one target, one drug” to “network target, multicomponent therapeutics”, highlighting a holistic view similar to that of traditional Chinese medicine.³⁰ The network pharmacology method, along with molecular docking, was used in this study to identify the active components, active targets, and potential mechanism of action of WLS to treat HUA. In addition, animal experiments were also conducted to validate the pharmacological effects of WLS.

Materials and Methods

Network Pharmacology Assay

Database and Software

The database and software for the assay of network pharmacology and molecular docking are listed in [Table 1](#).

Screening Active Compounds of WLS

The keywords “Fuling”, “Zhuling”, “Zexie”, “Baizhu”, and “Guizhi” were used to retrieve the compounds of WLS from the SymMap database and TCMSP database. The -cut-off values were oral bioavailability (OB) $\geq 30\%$ and drug-likeness (DL) ≥ 0.18 .⁴² A detailed description of the five herbs of WLS can be found in [Table 2](#) and [Figure 1A](#).

Compounds-Related Targets Prediction of WLS and Network Construction

The PubChem database and SwissTargetPrediction server were employed to obtain the canonical SMILES and predict the targets of the active compounds in WLS. The probability value of potential target proteins is ≥ 0.1 .⁴³ Cytoscape 3.9.0 was used to build a herb-active compound-target network.

Collection of HUA-Related Targets and Herb-Compound-Target-Disease Network Construction

The keywords “hyperuricemia” and “hyperuricaemia” were used to collect HUA-related targets through the OMIM database, GeneCards database, TTD database, DisGeNET database, and DrugBank database. We received an ethics committee waiver for using these five databases from the Medical and Animal Experiment Ethics Committee of Beijing University of Chinese Medicine. After deduplication/integration of data, crossover genes were obtained and considered as therapeutic targets relevant to HUA. The common targets of WLS for the treatment of HUA were generated by the Venn diagram. Moreover, a herb-compound-target-disease network was constructed by Cytoscape 3.9.0.

Table 1 Information on the Database and Software

Name	Website
Traditional Chinese Medicine Systems Pharmacology (TCMSP) database ³¹	https://old.tcm-sp-e.com/index.php
SymMap database ³²	http://www.symmap.org/
PubChem database ³³	https://pubchem.ncbi.nlm.nih.gov/
SwissTargetPrediction server ³⁴	http://www.swisstargetprediction.ch/
Online Mendelian Inheritance in Man (OMIM) database ³⁵	https://omim.org/
Therapeutic Target Database (TTD) ³⁶	http://db.idrblab.net/ttd/
DisGeNET database ³⁷	https://www.disgenet.org/
GeneCards database ³⁸	https://www.genecards.org/
DrugBank database ³⁹	https://go.drugbank.com/
Venny 2.1	https://bioinfogp.cnb.csic.es/tools/venny/index.html
STRING database ⁴⁰	https://cn.string-db.org/
Cytoscape 3.9.0 software	-
R 4.1.2	-
PDB database ⁴¹	http://www.rcsb.org/
AutoDockTools (1.5.7) software	-
OpenBabel (2.4.1) software	-
PyMOL (2.5.2) software	-

Table 2 Basic Information of Five Medicinal Materials of WLS

Chinese Name	English Name	Latin Name	Class in English
Zexie	Rhizome of Oriental Waterplantain	<i>Alismatis Rhizoma</i>	Diuretic Dampness Excreting Drugs
Fuling	Indian Bread	<i>Poria</i>	Diuretic Dampness Excreting Drugs
Zhuling	Polyporus Grifolia	<i>Polyporus</i>	Diuretic Dampness Excreting Drugs
Baizhu	Rhizome of Largehead Atractylodes	<i>Atractylodis Macrocephalae Rhizoma</i>	Qi Reinforcing Drugs
Guizhi	Cassia Twig	<i>Cinnamomi Ramulus</i>	Pungent-Warm Exterior-Releasing Medicinal

Construction of PPI Network

The intersection targets were imported into the STRING database. Then, the tabular text of the PPI network was imported into Cytoscape 3.9.0, and CytoNCA was used to filter the target genes.

The first filtration conditions consisted of Betweenness ≥ 47.69986603 , Closeness ≥ 0.475336323 , Degree ≥ 13 , Eigenvector ≥ 0.054424535 , LAC ≥ 6.444444444 , and Network ≥ 8.444444444 . The duplicate filtration conditions consisted of Betweenness ≥ 7.507037407 , Closeness ≥ 0.731707317 , Degree ≥ 19 , Eigenvector ≥ 0.177778021 , LAC ≥ 14.88888889 , and Network ≥ 16.39197012 . Finally, the filtered genes were used to construct the subnetwork, and the final network was subjected to duplicate filtering.

GO and KEGG Pathway Enrichment Analysis

First, R package “org.Hs.eg.db” was applied to eliminate errors caused by capitalization or abbreviations of the target name. Following that, GO biological functions and the KEGG pathway enrichment analysis were visualized using the R packages “DOSE” “clusterProfiler” and “pathview” for which the p-value was <0.05 , q-value <0.05 for further analysis. R software 4.1.2 was used to accomplish all preceding stages.

Molecular Docking Verification

In order to verify the binding ability of active compounds with key targets and explore their accurate binding modes, molecular docking simulation is done with the PDB database, PubChem database OpenBabel, AutoDockTools, and PyMOL software. Representative targets were chosen as receptors in the PPI network and representative therapeutic compounds were used as ligands. The 3D structures of IL6 (PDB ID = 5FUC), TNF (PDB ID = 5UUI), CASP3 (PDB ID = 5IBP), PPARG (PDB ID = 7E0A), and STAT3 (PDB ID = 6NJS) were downloaded from the PDB database. The SDF files with the 3D structure of ligand

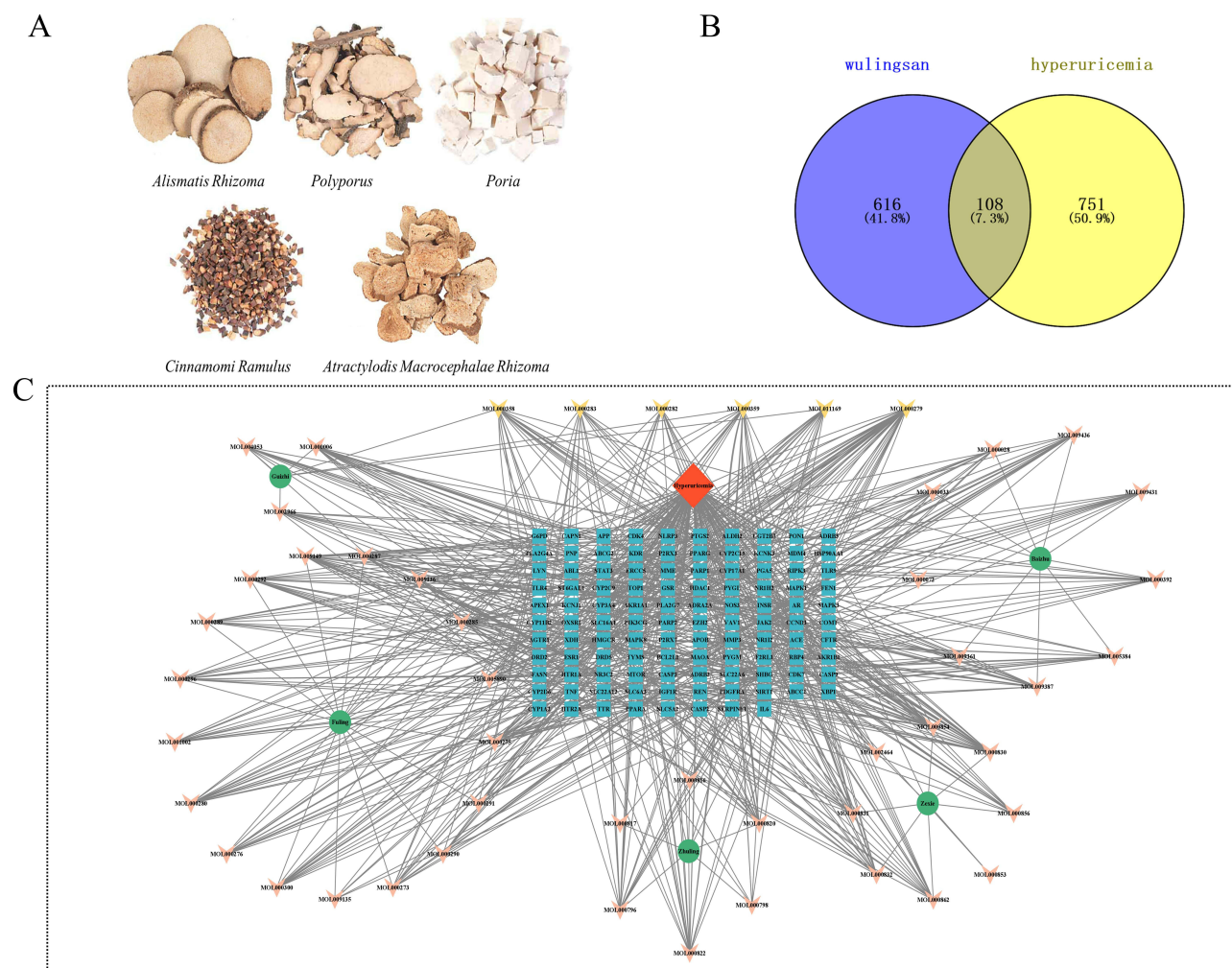


Figure 1 The network pharmacology of WLS in the treatment of HUA. **(A)** The five herbs of WLS. **(B)** The Venn diagram of WLS-HUA. **(C)** The herb-compound-target-disease network.

molecules were downloaded from the PubChem database. Using Open Babel 2.4.1, the structure files were translated to mol2 format. Molecular docking was carried out using AutoDocktools 4.0 after removing water molecules, adding nonpolar hydrogen, isolating proteins and calculating Gasteiger charges. PyMOL was then used to visualize the confirmation with the best affinity.

Experiment Validation

Experimental Drugs and Reagents

The Wuling San (capsule) and allopurinol were purchased from Jiangxi Pinxin Pharmaceutical Co., Ltd. (Xinyu, China) and Shanghai Xinyi Wanxiang Pharmaceutical Co., Ltd. (Shanghai, China), respectively. Potassium oxonate (PO) and sodium carboxymethyl cellulose (CMC-Na) were purchased from Yuanye Biological Co., Ltd. (Shanghai, China). Yeast extract was bought from OXOID Ltd. (Basingstoke, UK). UA content detection kit was purchased from BioSino Bio-Technology & Science Inc. (Beijing, China). Catalase (CAT) assay kit, total antioxidant capacity (T-AOC) assay kit, malondialdehyde (MDA) assay kit, superoxide dismutase (SOD) assay kit, creatinine (Cr) assay kit, and blood urea nitrogen (BUN) assay kit were purchased from Nanjing Jiancheng Bioengineering Institute (Nanjing, China). The kits for the detection of interleukin-6 (IL-6) and tumor necrosis factor- α (TNF- α) were bought from Neobioscience Technology Co., Ltd. (Shenzhen, China).

Animals and Treatment

Forty Specific Pathogen-Free (SPF) Sprague-Dawley (SD) male rats were purchased from SPF (Beijing) Biotechnology Co., Ltd (laboratory animal license number: SCXK (Jing) 2020-0033). Before the experiments, the rats were acclimated for one week to

the experimental conditions (temperature: $22 \pm 2^\circ\text{C}$; 12h dark-light cycle; humidity $50 \pm 10\%$) and were fed a standard diet with free access to water. The Ethics Committee of Beijing University of Chinese Medicine approved all proposals involving animals (BUCM-4-2022022802-1026) and the experimental procedures were carried out in accordance with the Guidelines on the Care and Use of Laboratory Animal issued by the Chinese Council on Animal Research and the Guidelines of Animal Care.

The rats were randomly divided into five groups (each group of 8): blank control (BC) group; model control (MC) group; Allopurinol (ALL) group (10mg/kg/d); Wuling San high-dose group (WLS-HD, 630mg/kg/d); Wuling San low-dose group (WLS-LD, 315mg/kg/d). Potassium oxonate, Allopurinol, and Wuling San (capsule) were suspended in the 0.5% CMC-Na solution, respectively. The yeast extract was dissolved in pure water. In order to induce HUA, all groups except the BC group were intragastrically given PO (750 mg/kg /d) for 14 days. The model group was given 0.5% CMC-Na, the ALL group was given allopurinol treatment, and the WLS groups were given different WLS treatments via gavage, respectively. In contrast, the BC group received 0.5% CMC-Na in comparable volumes. In order to simulate the purine metabolism disorder caused by human consumption of high-purine food and increase UA levels, all groups except the BC group were intragastrically given yeast extract (10g/kg/d) on the same day; meanwhile, the BC group received pure water in comparable volumes.

Sample Collection

All rats were sacrificed under anesthesia at 2 h after the last treatment administration, and whole blood samples were quickly taken via the abdominal aorta. Then the blood samples were centrifuged (3500 rpm for 10min at 4°C), and the serum was stored at -80°C until further analysis.

Determination of Biochemical Indexes in HUA Rats

The serum levels of UA (SUA), Cr (SCr), and BUN levels were measured using commercial kits, following the manufacturer's instructions.

Determination of Oxidative Stress in HUA Rats

The levels of T-AOC, SOD, CAT, and MDA in serum were evaluated using commercial kits, as directed by the manufacturer.

Determination of Inflammatory Factors in HUA Rats

In accordance with the instructions, the contents of IL-6 and TNF- α in serum were measured by using an ELISA kit.

Statistical Analysis

All data were expressed as mean \pm standard deviation (mean \pm SD). One-way ANOVA followed by LSD post hoc test was performed for comparisons of data. For all statistical tests, $P < 0.05$ was considered statistically significant. The analysis was performed using IBM SPSS 25.0 (Armonk, NY, USA) and GraphPad Prism 8 (San Diego, California, USA).

Results

Network Pharmacology Assay

Active Compounds and Targets Prediction and Herb-Compound-Target Network Construction

A total of 55 active compounds of WLS were screened, among which 10 were from Baizhu, 20 were from Fuling, 6 were from Guizhi, 9 were from Zexie, and 10 were from Zhuling. Next, according to the active compounds, 3622 related targets of WLS were identified by SwissTargetPrediction, containing 718 types in Baizhu, 1336 types in Fuling, 324 types in Guizhi, 696 types in Zexie, and 548 types in Zhuling. After the elimination of redundancy, 49 compounds and 724 targets were identified and used to build the herb-active compound-target network, which contained 778 nodes and 3677 edges, five of which were Chinese herbal medicine nodes. Forty-nine active compound nodes and 724 target genes were unique to the herbs as shown in [Table 3](#) and [Supplementary Figure 1](#).

Putative Targets of WLS for Treating HUA

HUA-related targets were searched in OMIM, DrugBank, DisGeNET, TTD, and GeneCards databases. 5, 69, 196, 5 and 763 targets were identified in OMIM, DrugBank, DisGeNET, TTD, and GeneCards databases, respectively. After removing the redundancies, a total of 859 HUA-related targets were obtained. Subsequently, 108 overlapping targets of WLS and HUA were screened via Venny 2.1 as depicted in [Figure 1B](#).

Table 3 Information on Active Compounds of WLS

No.	Herb	Mol ID	Molecule Name	OB (%)	DL
1	Guizhi	MOL000006	Luteolin	36.16	0.25
2	Baizhu	MOL000028	A-Amyrin	39.51	0.76
3	Baizhu	MOL000033	(3S,8S,9S,10R,13R,14S,17R)-10,13-Dimethyl-17-[(2R,5S)-5-Propan-2-Yloctan-2-Yl]-2,3,4,7,8,9,11,12,14,15,16,17-Dodecahydro-1H-Cyclopenta[A]Phenanthren-3-Ol	36.23	0.78
4	Baizhu	MOL000072	8B-Ethoxy Atractylenolide III	35.95	0.21
5	Fuling	MOL000273	(2R)-2-[(3S,5R,10S,13R,14R,16R,17R)-3,16-Dihydroxy-4,4,10,13,14-Pentamethyl-2,3,5,6,12,15,16,17-Octahydro-1H-Cyclopenta[A]Phenanthren-17-Yl]-6-Methylhept-5-Enoic Acid	30.93	0.81
6	Fuling	MOL000275	Trametenolic Acid	38.71	0.8
7	Fuling	MOL000276	7,9(11)-Dehydropachymic Acid	35.11	0.81
8	Fuling, Zhuling	MOL000279	Cerevisterol	37.96	0.77
9	Fuling	MOL000280	(2R)-2-[(3S,5R,10S,13R,14R,16R,17R)-3,16-Dihydroxy-4,4,10,13,14-Pentamethyl-2,3,5,6,12,15,16,17-Octahydro-1H-Cyclopenta[A]Phenanthren-17-Yl]-5-Isopropyl-Hex-5-Enoic Acid	31.07	0.82
10	Fuling, Zhuling	MOL000282	Ergosta-7,22E-Dien-3Beta-Ol	43.51	0.72
11	Fuling, Zhuling	MOL000283	Ergosterol Peroxide	40.36	0.81
12	Fuling	MOL000285	(2R)-2-[(5R,10S,13R,14R,16R,17R)-16-Hydroxy-3-Keto-4,4,10,13,14-Pentamethyl-1,2,5,6,12,15,16,17-Octahydrocyclopenta[A]Phenanthren-17-Yl]-5-Isopropyl-Hex-5-Enoic Acid	38.26	0.82
13	Fuling	MOL000287	3Beta-Hydroxy-24-Methylene-8-Lanostene-21-Oic Acid	38.70	0.81
14	Fuling	MOL000289	Pachymic Acid	33.63	0.81
15	Fuling	MOL000290	Poricoic Acid A	30.61	0.76
16	Fuling	MOL000291	Poricoic Acid B	30.52	0.75
17	Fuling	MOL000292	Poricoic Acid C	38.15	0.75
18	Fuling	MOL000296	Hederagenin	36.91	0.75
19	Fuling	MOL000300	Dehydroeburicoic Acid	44.17	0.83
20	Baizhu, Guizhi	MOL000358	Beta-Sitosterol	36.91	0.75
21	Zexie, Guizhi	MOL000359	Sitosterol	36.91	0.75
22	Baizhu	MOL000392	Formononetin	69.67	0.21
23	Zhuling	MOL000796	(22E,24R)-Ergosta-6-En-3Beta,5Alpha,6Beta-Triol	30.20	0.76
24	Zhuling	MOL000798	Ergosta-7,22-Diene-3B-Ol	43.51	0.72
25	Zhuling	MOL000816	Ergosta-7,22-Dien-3-One	44.88	0.72
26	Zhuling	MOL000817	Ergosta-5,7,22-Trien-3-Ol	46.18	0.72
27	Zhuling	MOL000820	Polyporusterone E	45.71	0.85
28	Zhuling	MOL000822	Polyporusterone G	33.43	0.81
29	Zexie	MOL000830	Alisol B	34.47	0.82
30	Zexie	MOL000831	Alisol B monoacetate	35.58	0.81
31	Zexie	MOL000832	Alisol,b,23-acetate	32.52	0.82
32	Zexie	MOL000853	Alisol B	36.76	0.82
33	Zexie	MOL000854	Alisol C	32.70	0.82
34	Zexie	MOL000856	Alisol C monoacetate	33.06	0.83
35	Zexie	MOL000862	[(1S,3R)-1-[(2R)-3,3-dimethyloxiran-2-yl]-3-[(5R,8S,9S,10S,11S,14R)-11-hydroxy-4,4,8,10,14-pentamethyl-3-oxo-1,2,5,6,7,9,11,12,15,16-decahydrocyclopenta[a]phenanthren-17-yl]butyl] acetate	35.58	0.81
36	Fuling	MOL001002	Ellagic Acid	43.06	0.43
37	Zexie	MOL002464	1-Monolinolein	37.18	0.3
38	Guizhi	MOL002966	Dalbergin	78.18	0.2
39	Guizhi	MOL004053	Isodalbergin	35.45	0.2
40	Baizhu	MOL005384	Suchilactone	57.52	0.56
41	Fuling	MOL005890	Pachypodol	75.06	0.4
42	Fuling	MOL009135	Ellipticine	30.82	0.28
43	Fuling	MOL009136	Peraksine	82.58	0.78
44	Fuling	MOL009149	Cheilanthifoline	46.51	0.72

(Continued)

Table 3 (Continued).

No.	Herb	Mol ID	Molecule Name	OB (%)	DL
45	Baizhu	MOL009361	13,15-Dideoxyaconitine	34.67	0.25
46	Baizhu	MOL009387	Didehydrotuberostemonine	51.91	0.74
47	Baizhu	MOL009431	Stemonine	81.75	0.72
48	Baizhu	MOL009436	Stemotinine	38.69	0.46
49	Zhuling, Guizhi	MOL011169	Peroxyergosterol	44.39	0.82

Construction of the Herb-Compound-Target-Disease Network

The herb-compound-target-disease network contained 163 nodes and 820 edges, among which 5 were Chinese herbal medicine nodes, 49 were active compound nodes, 108 were target genes and one was a disease as presented in [Figure 1C](#).

PPI Network Construction and Analysis

The 108 common target genes were input into the STRING 11.0 platform to construct the PPI network. A confidence score ≥ 0.4 was selected, and the nodes that disconnected from the network were hidden. The PPI network was exported as a tab-separated values (TSV) file and visualized using Cytoscape software (version 3.9.0). By setting the DC, BC, NC, EC, and LAC values to be greater than the median, two screenings were performed and 12 core network genes were finally screened out. As shown in [Figure 2A](#), there were 107 nodes and 913 edges in the interaction network. The core network genes screened out included TNF, IL6, CASP3, MTOR, PPARG, HSP90AA1, STAT3, PTGS2, MAPK3, ESR1, SIRT1, NOS3, and these genes made up the core nodes in the PPI network ([Figure 2B](#)).

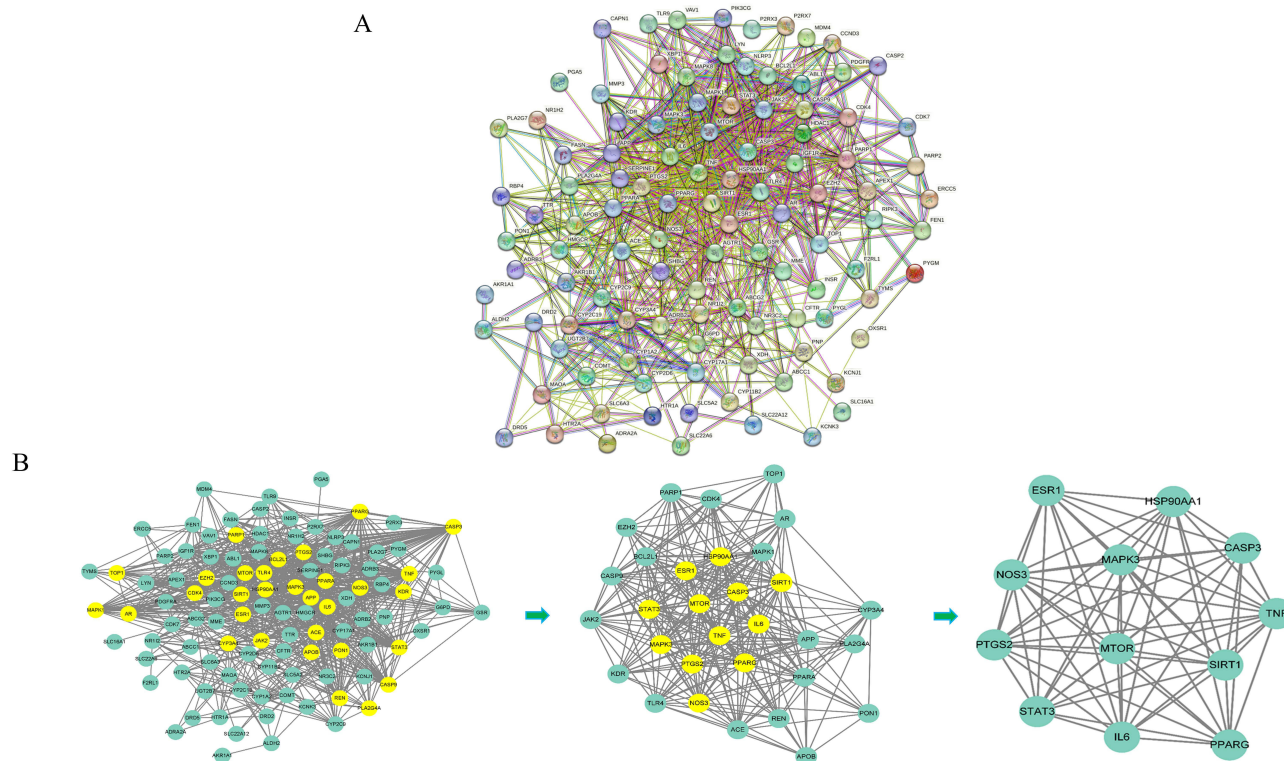


Figure 2 The protein-protein interaction network of WLS in the treatment of HUA targets and analysis of CytoNCA core network. (A) Protein-protein interaction network. (B) Subnetwork topology analysis diagram. Yellow nodes are the core genes obtained after screening.

GO and KEGG Pathway Enrichment Analysis

As a part of GO analysis, biological process (BP), cellular components (CC), and molecular function (MF) were included, and 1981 terms were derived via BP enrichment analysis (including cellular response to chemical stress, steroid metabolic process, response to lipopolysaccharide, response to oxidative stress); 55 terms via CC enrichment analysis (including membrane raft, membrane microdomain, caveola, plasma membrane raft, nuclear envelope); 147 terms via MF enrichment analysis (including oxidoreductase activity, nuclear receptor activity, ligand-activated transcription factor activity, steroid hydroxylase activity, and heme-binding). The top 10 BP, CC, and MF were selected to draw the GO function histogram of WLS in HUA treatment. Results showed that WLS was involved in the treatment of HUA through a variety of gene biological functions (Figure 3). To further clarify the pathways regulated by the therapeutic target genes, we performed a KEGG pathway analysis. Results showed that these target genes were distributed in 155 pathways. In order to build a histogram, the pathways containing the top 30 enriched genes were selected. HUA-related pathways were largely involved in HIF-1, PI3K-Akt, IL-17, TNF, and NOD-like receptor signaling pathways as depicted in Figure 4, [Supplementary Figures 2](#) and [3](#).

Molecular Docking Verification

After checking related published literature, the five core proteins, IL6, TNF, CASP3, PPARG, and STAT3 and the best effective ingredients, cerevisterol, luteolin, ergosterol peroxide, beta-sitosterol, and sitosterol, were selected for molecular docking. The molecular docking confirmed that the active ingredients of WLS had significant regulatory effects on IL-6, TNF, CASP3,

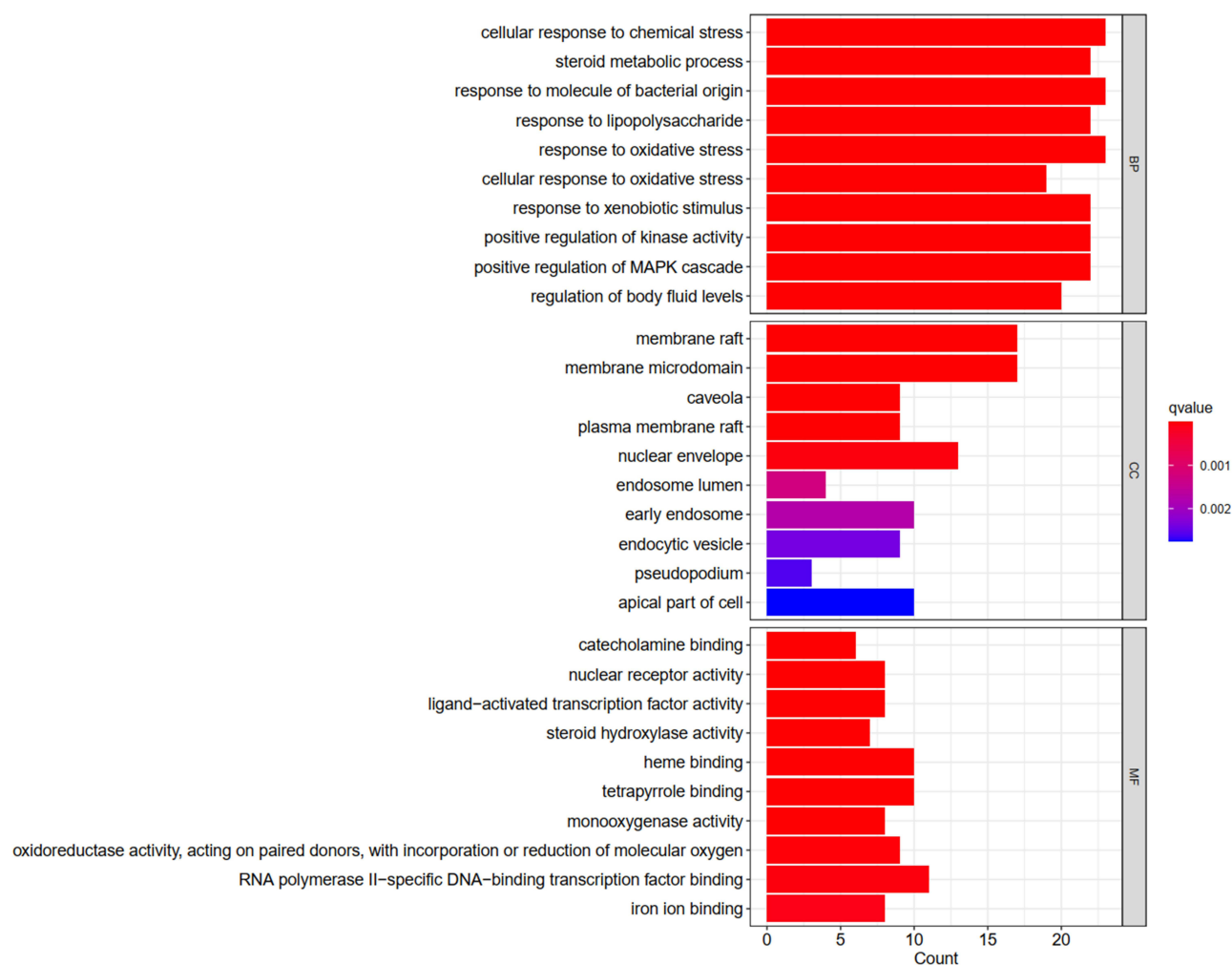


Figure 3 GO function enrichment analysis in HUA treated with WLS.

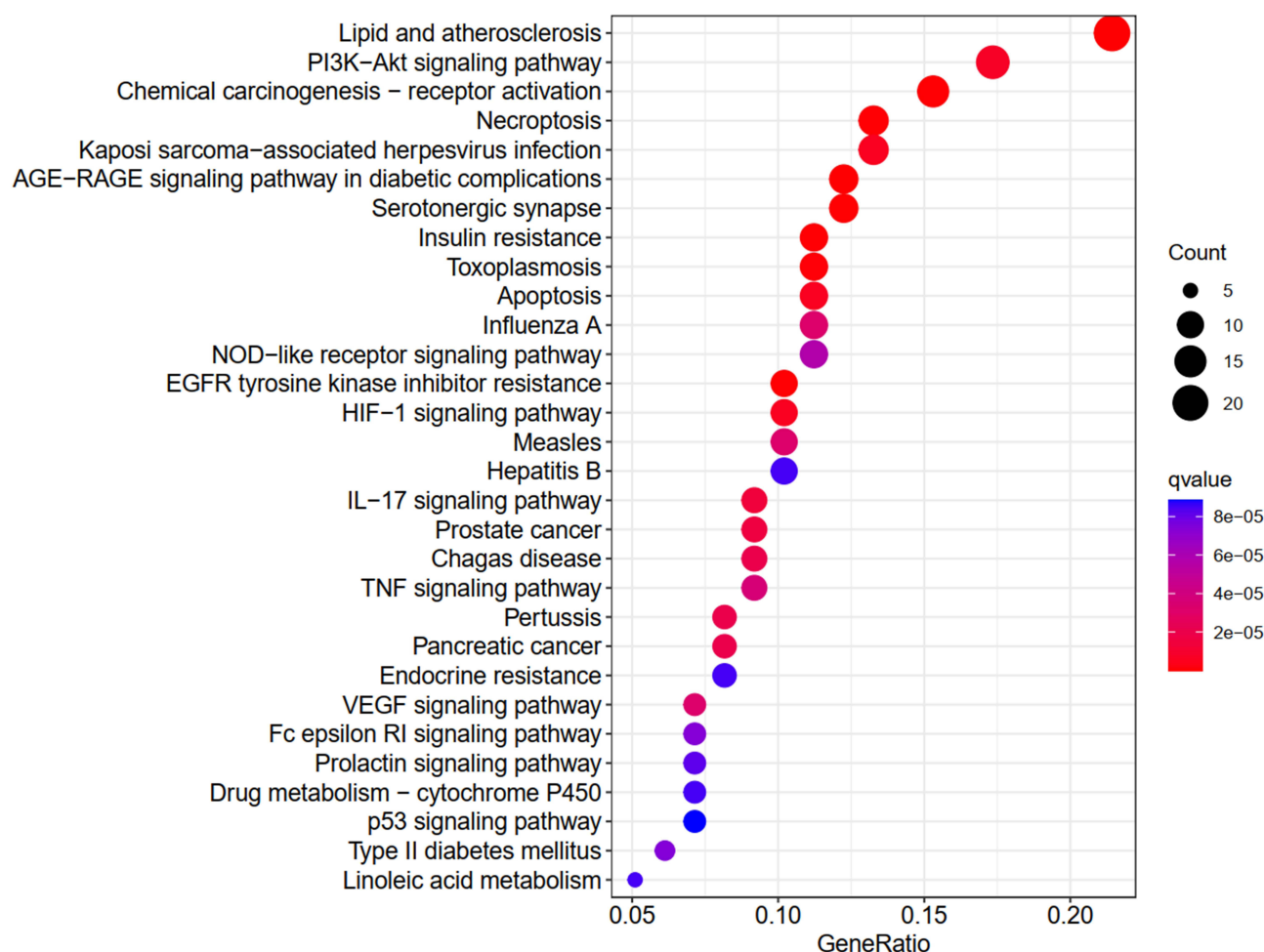


Figure 4 KEGG pathway enrichment analysis in HUA treated with WLS.

PPARG, and STAT3 as depicted in [Figure 5](#), [Supplementary Figures 4-6](#). As presented in [Table 4](#), the absolute values of the binding energies between active ingredients and core proteins were all greater than five, indicating that the key active ingredients of WLS had a strong affinity with the core proteins IL6, TNF, CASP3, PPARG, and STAT3, and all of which may play a key role in the treatment of HUA.

Validation of Animal Experiment

Effects of WLS on Biochemical Indexes in HUA Rats

Throughout the entire experimental period, the rats were in good health. There was no significant difference in body weight among the five groups as presented in [Figure 6A](#). The SUA level of the MC group was significantly higher than that of the BC group ($P < 0.01$) as shown in [Figure 6B](#), indicating that the HUA rat model was successfully constructed. As shown in [Figure 6C](#) and [D](#), the levels of SCr and BUN in the MC group were slightly higher than those in the BC group, but there was no statistical significance. SUA level significantly decreased in ALL and different doses of WLS group compared to the level in MC group ($P < 0.01$). In comparison with MC group, levels of SCr and BUN decreased in all treatment groups, but this difference was not statistically significant.

Effect of WLS on Antioxidative Stress Ability in HUA Rats

As shown in [Figure 7A](#), the level of MDA was significantly increased in the serum of MC group compared with the BC group ($p < 0.01$). The levels of SOD ([Figure 7B](#)) and T-AOC ([Figure 7C](#)) were significantly decreased in the serum of MC group compared with the BC group ($p < 0.01$). Although the level of CAT was decreased in the MC group compared with

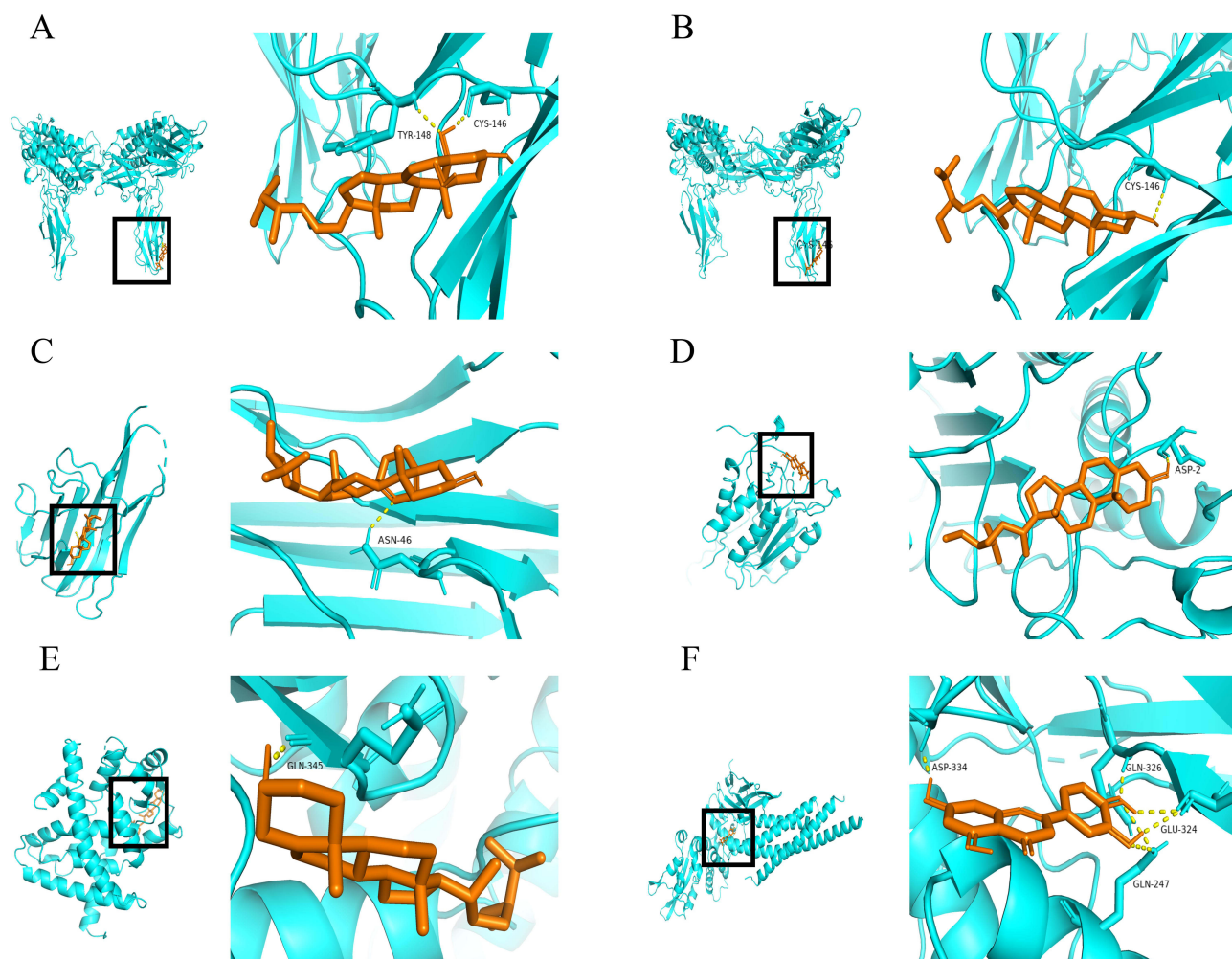


Figure 5 Part of molecular docking results. (A) IL6 and Cerevisterol. (B) IL6 and Beta-Sitosterol. (C) TNF and Ergosterol Peroxide. (D) CASP3 and Beta-Sitosterol. (E) PPARG and Sitosterol. (F) STAT3 and Luteolin.

the BC group, it was not statistically significant (Figure 7D). Compared with the MC group, the level of MDA in the serum of WLS-HD was significantly decreased ($p < 0.01$), and the levels of SOD and T-AOC in the serum of ALL, WLS-LD, and WLS-HD groups were significantly increased ($p < 0.01$), which indicated that WLS could improve oxidative stress in HUA rat model.

Determination of Inflammatory Factors in Rats Model of HUA

As shown in Figure 8A and B, the contents of IL-6 and TNF- α in the serum of MC group were significantly increased compared with the BC group ($p < 0.01$). Compared with the MC group, the TNF- α and IL-6 contents in the serum of ALL,

Table 4 Binding Energy of Active Compounds in WLS with Potential HUA Targets

Active Compounds	Binding Energy (kcal/mol)				
	IL6 (5FUC)	TNF (5UUI)	CASP3 (5IBP)	PPARG (7E0A)	STAT3 (6NJS)
Beta-Sitosterol	-7.24	-7.00	-8.41	-9.10	-6.60
Cerevisterol	-7.65	-7.59	-7.49	-10.03	-6.97
Ergosterol Peroxide	-6.49	-7.91	-8.85	-10.35	-6.94
Luteolin	-5.23	-6.86	-6.04	-7.82	-5.12
Sitosterol	-6.60	-7.43	-7.91	-8.97	-6.79

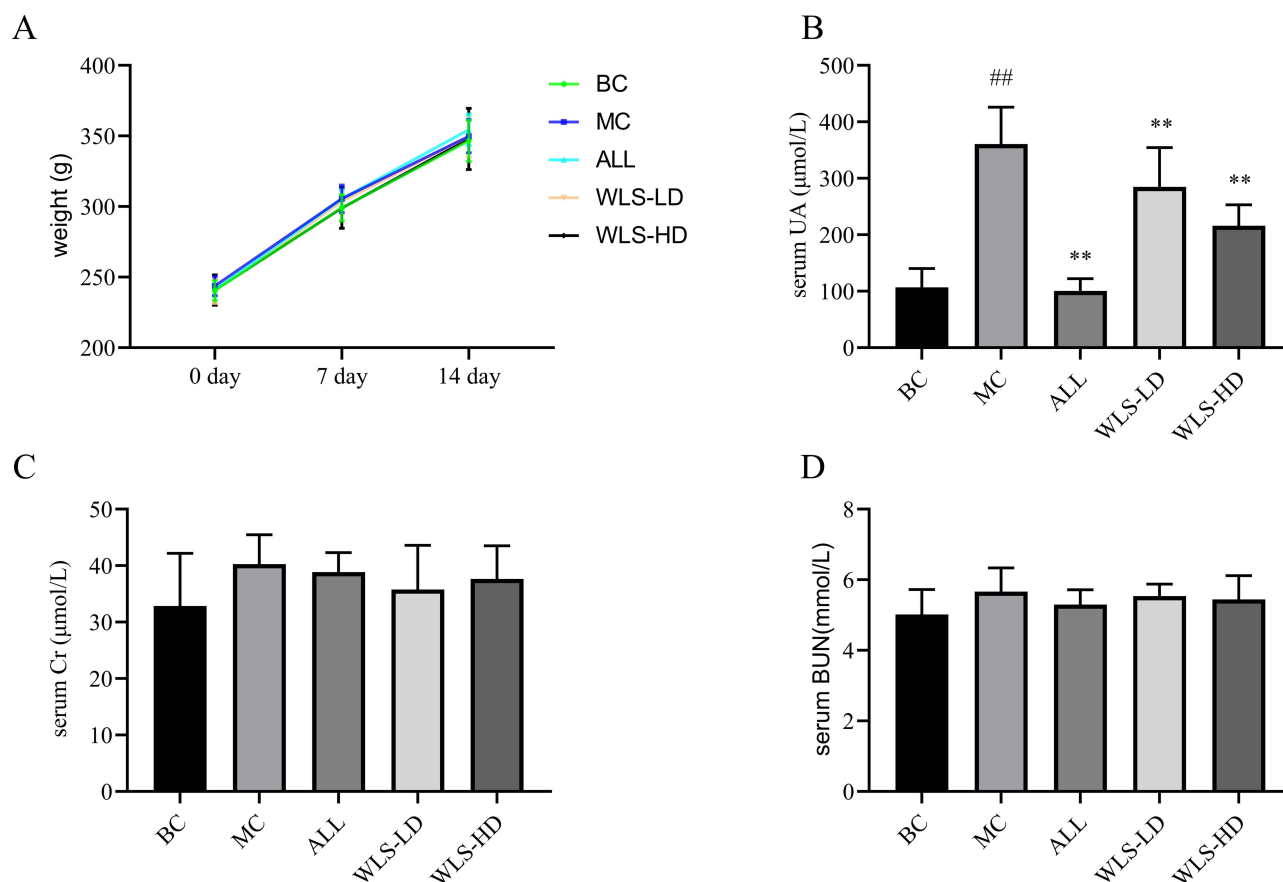


Figure 6 The effect of WLS on body weight (A), SUA (B), SCr (C), and BUN (D) in HUA rats. Compared with the BC group, ^{###} $p < 0.01$; Compared with the MC group, ^{**} $p < 0.01$.

WLS-LD, and WLS-HD groups were significantly reduced ($p < 0.01$), which indicated that WLS could improve inflammation levels and exert anti-inflammatory effects in the HUA rat model.

Discussion

There has been a dramatic upward trend in the prevalence of HUA and gout in recent years.^{44–46} The most common drugs used for treating HUA are uricostatic agents (allopurinol and febuxostat), which decrease the production of UA by competing with XO, and uricosuric agents (probenecid and benzbromarone) which modulate the renal tubular reabsorption of UA by increasing the renal clearance of UA in the kidney.⁴⁷ However, these medications can cause some undesired side effects such as hypersensitivity reactions, gastrointestinal discomfort, and drug-drug interactions.⁴⁸ WLS, a traditional Chinese medicine preparation, has been used for thousands of years to treat diseases related to humoral balance. It has been previously reported that WLS has the function of preventing calcium oxalate nephrolithiasis and has a positive effect on diuresis.^{49,50} As to the treatment of HUA, studies also have shown that WLS can effectively inhibit TLR4/MyD88 signaling and NLRP3 inflammasome activity, which reduces IL-1 β production and modulates renal organic ion transporters in hyperuricemic mice fed with high fructose.²⁶ However, there is little understanding of the active compounds of this traditional herbal formula against HUA. In this study, we explored the active compounds of WLS and the HUA treatment-related molecular targets, as well as the molecular mechanism of WLS in the treatment of HUA based on network pharmacology.

In this study, 49 compounds and 108 core targets of WLS for the treatment of HUA were screened out. According to the compound-target regulatory network, cerevisterol, luteolin, ergosterol peroxide, beta-sitosterol, sitosterol, and other active compounds could act on multiple targets. Cerevisterol and ergosterol peroxide are both the active compound of

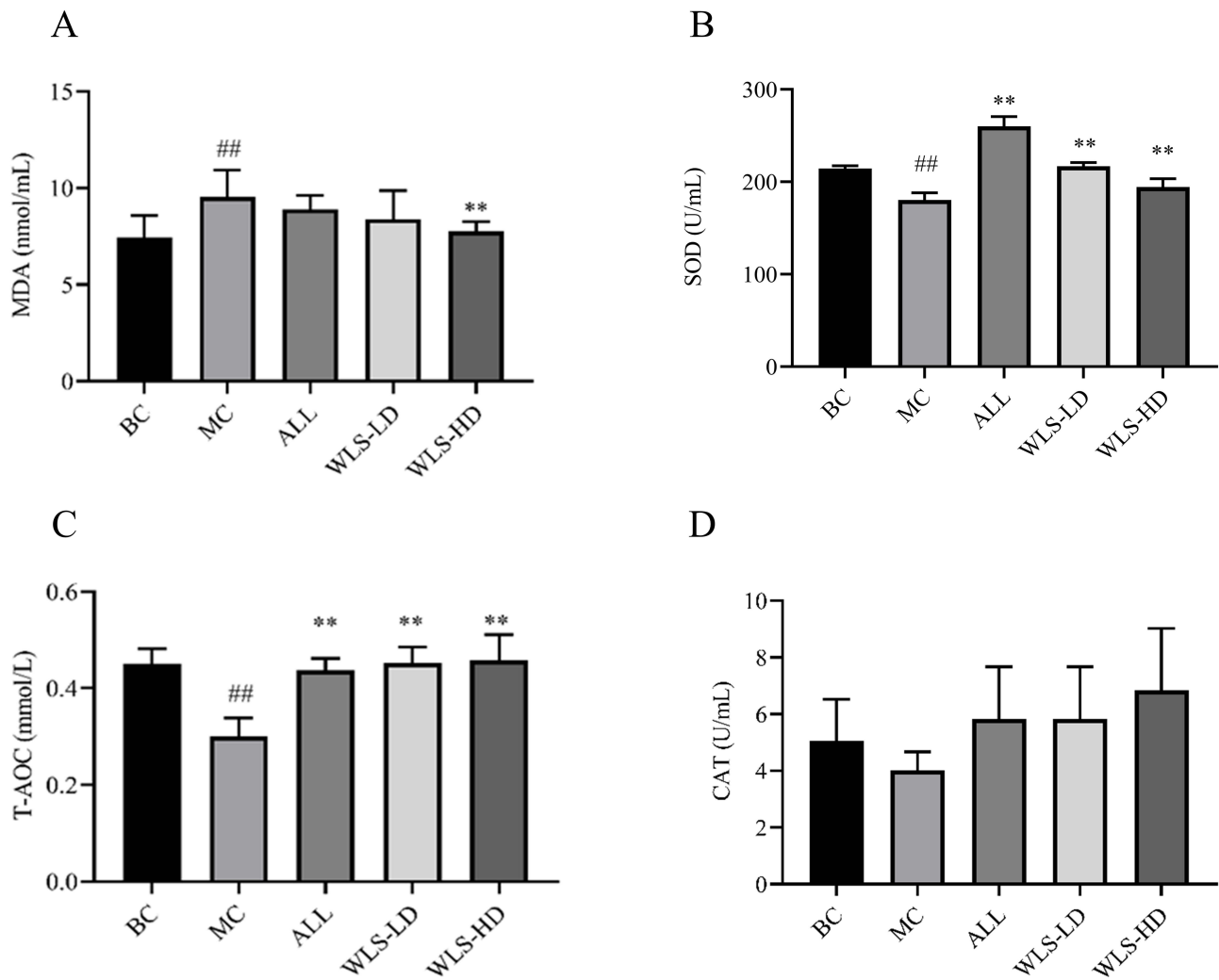


Figure 7 The effect of WLS on the levels of MDA (A), SOD (B), T-AOC (C), and CAT (D) in HUA rats. Compared with the BC group, ^{##} $p < 0.01$; Compared with the MC group, ^{**} $p < 0.01$.

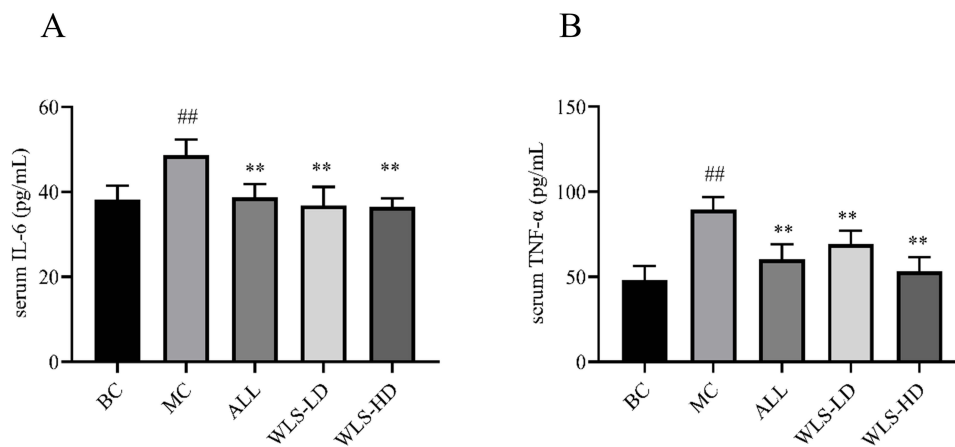


Figure 8 The effect of WLS on the contents of IL-6 (A) and TNF-α (B) in HUA rats. Compared with the BC group, ^{##} $p < 0.01$; Compared with the MC group, ^{**} $p < 0.01$.

Poria (Fuling) and *Polyporus* (Zhuling), luteolin is the active compound of *Cinnamomi Ramulus* (Guizhi), beta-sitosterol is the active compound of *Atractylodis Macrocephalae Rhizoma* (Baizhu) and *Cinnamomi Ramulus* (Guizhi), sitosterol is the active compound of *Alismatis Rhizoma* (Zexie) and *Cinnamomi Ramulus* (Guizhi). All four compounds, except luteolin, are the active compounds of two traditional Chinese medicines, similar to how traditional Chinese medicines work together in synergy and compatibility. In previous studies, these potential active compounds in WLS were found to inhibit inflammation, improve oxidative stress, and lower SUA levels. Cerevisterol can decrease the expression of pro-inflammatory cytokines, such as TNF- α , IL-6, and IL-1 β in LPS-induced macrophages via deactivating NF- κ B and AP-1 transcription factors through the down-regulation of MAPK signaling, and the up-regulation of Nrf2-mediated HO-1 expression, suggesting the potential of cerevisterol as an anti-inflammatory agent.⁵¹ Luteolin is a natural flavonoid that possesses strong anti-oxidative and anti-inflammatory properties. Studies have shown that luteolin can contribute to reducing tissue UA levels in the liver, decreasing neutrophil infiltration and pro-inflammatory cytokines production, and it also is able to reduce oxidative stress in MSU crystal-induced inflammation and has the protective effects on kidneys.^{52,53} Ergosterol peroxide has antiviral and immunomodulatory abilities, evidenced by the finding that ergosterol peroxide can suppress LPS-induced TNF- α production by inhibiting the activation of the MAPKs and transcription factor NF- κ B and C/EBP in RAW264.7 cells.^{54,55} Beta-sitosterol can suppress the paw swelling caused by MSU crystals injection, indicating its anti-inflammatory properties.⁵⁶

In the current study, the PPI analysis showed that TNF, IL6, CASP3, PPARG, STAT3, MTOR, HSP90AA1, PTGS2, MAPK3, ESR1, SIRT1, and NOS3 are the core targets involved in the treatment of HUA by WLS. Moreover, GO enrichment analysis indicated that WLS might interfere with oxidative stress in the treatment of HUA, and KEGG enrichment analysis indicated multiple inflammation-related signaling pathways, including TNF, and NOD-like receptor, HIF-1, PI3K-Akt, and IL-17 signaling pathways. UA is the final oxidation product of purine metabolism in the circulatory system, which is thought to contribute to the development of gout. In addition, epidemiological and experimental studies have reported that HUA is strongly related to an increased risk for cardiovascular disease, metabolic syndrome (MS), stroke, and CKD. All these conditions are thought to be possibly mediated by oxidative stress and a pro-inflammatory milieu.^{57,58} In previous studies, researchers demonstrated that the serum levels of MDA, IL-6, TNF- α , and IL-8 in asymptomatic young patients with HUA were significantly higher than healthy counterparts,⁵⁹⁻⁶¹ and patients with high levels of UA had higher inflammation and oxidative stress. UA can stimulate TNF- α production in a dose-dependent manner,⁶² and it has been proved that TNF- α exposure before MSU stimulation can result in the release of IL-1 β from human neutrophils.⁶³ Similarly, priming of human neutrophils with IL-6 stimulates UA-mediated IL-1 β secretion, suggesting that IL-6 plays a role in MSU-mediated NLRP3 inflammasome activation.⁶⁴ ROS induced by UA can activate the cleavage of caspase-3 and downregulate the expression of the Bcl-xl via the caspase-dependent apoptosis pathway in NRK-52E cells.⁶⁵ In HUVECs, UA can upregulate JAK2/STAT3 in a concentration-dependent manner, as well as the pro-inflammatory cytokine IL-6.⁶⁶ Additionally, previous studies showed that a relatively high concentration of UA can boost the expression of GLUT9 and URAT1 in renal tubular epithelial cells by activating the JNK, NF- κ B, and PI3K/Akt signaling pathways.⁶⁷ An upregulation of HIF-1 α with UA stimulation in HAEC was reported by Oberbach.⁶⁸ Correspondingly, there are many drugs targeting UA to exert their therapeutic effect. Arhalofenate, a partial agonist of PPARG (peroxisome proliferator-activated receptor-gamma), inhibits UA transport and has anti-inflammation properties,⁶⁹ and rosiglitazone (a PPARG agonist) can attenuate the hyperuricemic nephropathy through suppressing inflammation and lowering SUA levels by preserving the expression of urate transporters.⁷⁰ All of these findings related to UA-induced oxidative stress and inflammation prove to play a crucial role in the development of HUA, which gives us insight that in addition to urate-lowering therapies, anti-inflammatory, and anti-oxidative stress therapies may also be helpful in the treatment of HUA.

In the validation experiment, the HUA rat model was established by oral administration of PO and yeast extract to further ascertain whether WLS was able to lower the level of UA. The results showed that compared with the HUA group, the WLS groups had a significant reduction in the level of SUA. In the present study, PO and yeast extract by gavage for 14 days induced HUA, but the changes in renal function indicators were not significant. In the meantime, the intervention of WLS was able to lower the SUA without affecting renal function.

As already mentioned above, an increase in SUA could contribute to oxidative and inflammation. In this work, a significant increase in SOD and T-AOC levels, accompanied by a decrease in MDA level in serum was observed after

WLS treatment. Moreover, WLS was found to decrease the contents of TNF- α and IL-6 in the serum. Therefore, it was suggested that WLS had the effect of improving oxidative stress and anti-inflammatory function in the HUA rat model.

There are some limitations in the present study. First, the active compounds of WLS are predicted based on five single traditional Chinese medicines rather than the whole formula, which may contribute to deviation from the realistic compounds. Second, the basis that WLS can treat HUA is that it contains a variety of compounds. However, it is hard to clarify the concrete roles that those compounds play in the treatment of HUA. Therefore, we will focus more on experiments to explore the mechanisms of key compounds in WLS on HUA in the future.

Conclusions

In summary, WLS has the characteristics of multicomponent, multitarget, and multipathways when it comes to treating HUA. It is mainly involved in controlling the development of HUA via inflammation-related signaling pathways, including TNF, NOD-like receptor, HIF-1, PI3K-Akt, IL-17 signaling pathways, and other signaling pathways. The analysis demonstrated that WLS could improve oxidative stress. The inhibiting inflammatory factors, such as TNF- α and IL-6, may also be one of its mechanisms. This study suggests a possible mechanism and potential clinical application values of WLS in the treatment of HUA and its related complications.

Data Sharing Statement

The data used to support the findings of this study are included in the article.

Author Contributions

All authors made a significant contribution to the work reported, whether that is in the conception, study design, execution, acquisition of data, analysis and interpretation, or in all these areas; took part in drafting, revising or critically reviewing the article; gave final approval of the version to be published; have agreed on the journal to which the article has been submitted; and agree to be accountable for all aspects of the work.

Funding

This work was funded by the National Natural Science Foundation of China (No. U20A20406).

Disclosure

The authors declare that there is no conflict of interest regarding the publication of this paper.

References

1. Huang J, Ma ZF, Zhang Y, et al. Geographical distribution of hyperuricemia in mainland China: a comprehensive systematic review and meta-analysis. *Glob Health Res Policy*. 2020;5(1):52. doi:10.1186/s41256-020-00178-9
2. Qian T, Sun H, Xu Q, et al. Hyperuricemia is independently associated with hypertension in men under 60 years in a general Chinese population. *J Hum Hypertens*. 2021;35(11):1020–1028. doi:10.1038/s41371-020-00455-7
3. Welnicki M, Gorczyca I, Wójcik W, et al. Hyperuricemia as a Marker of Reduced Left Ventricular Ejection Fraction in Patients with Atrial Fibrillation: results of the POL-AF Registry Study. *J Clin Med*. 2021;10(9):1829. doi:10.3390/jcm10091829
4. Oh TR, Choi HS, Kim CS, et al. Hyperuricemia has increased the risk of progression of chronic kidney disease: propensity score matching analysis from the KNOW-CKD study. *Sci Rep*. 2019;9(1):6681. doi:10.1038/s41598-019-43241-3
5. Hussain M, Elahi A, Hussain A, Iqbal J, Akhtar L, Majid A. Sodium-Glucose Cotransporter-2 (SGLT-2) Attenuates Serum Uric Acid (SUA) Level in Patients with Type 2 Diabetes. *J Diabetes Res*. 2021;2021:9973862. doi:10.1155/2021/9973862
6. Song P, Wang H, Xia W, Chang X, Wang M, An L. Prevalence and correlates of hyperuricemia in the middle-aged and older adults in China. *Sci Rep*. 2018;8(1):4314. doi:10.1038/s41598-018-22570-9
7. Hou YL, Yang XL, Wang CX, Zhi LX, Yang MJ, You CG. Hypertriglyceridemia and hyperuricemia: a retrospective study of urban residents. *Lipids Health Dis*. 2019;18(1):81. doi:10.1186/s12944-019-1031-6
8. Chen WY, Fu YP, Zhou M. The bidirectional relationship between metabolic syndrome and hyperuricemia in China: a longitudinal study from CHARLS. *Endocrine*. 2022;76(1):62–69. doi:10.1007/s12020-022-02979-z
9. Catanzaro R, Sciuto M, He F, Singh B, Marotta F. Non-alcoholic fatty liver disease: correlation with hyperuricemia in a European Mediterranean population. *Acta Clin Belg*. 2022;77(1):45–50. doi:10.1080/17843286.2020.1783907
10. Doehner W, Landmesser U. Xanthine oxidase and uric acid in cardiovascular disease: clinical impact and therapeutic options. *Semin Nephrol*. 2011;31(5):433–440. doi:10.1016/j.semnephrol.2011.08.007

11. Hussain T, Tan B, Yin Y, Blachier F, Tossou MC, Rahu N. Oxidative Stress and Inflammation: what Polyphenols Can Do for Us? *Oxid Med Cell Longev*. 2016;2016:7432797. doi:10.1155/2016/7432797
12. Elgebaly HA, Germoush MO, et al. A flavonoid-rich fraction of *Monolluma quadrangula* inhibits xanthine oxidase and ameliorates potassium oxonate-induced hyperuricemia in rats. *Environ Sci Pollut Res Int*. 2022;29(42):63520–63532. doi:10.1007/s11356-022-20274-2
13. Deng Y, Liu F, Yang X, Xia Y. The Key Role of Uric Acid in Oxidative Stress, Inflammation, Fibrosis, Apoptosis, and Immunity in the Pathogenesis of Atrial Fibrillation. *Front Cardiovasc Med*. 2021;8:641136. doi:10.3389/fcvm.2021.641136
14. Maharani N, Kuwabara M, Hisatome I. Hyperuricemia and Atrial Fibrillation. *Int Heart J*. 2016;57(4):395–399. doi:10.1536/ihj.16-192
15. Albu A, Para I, Porojan M. Uric Acid and Arterial Stiffness. *Ther Clin Risk Manag*. 2020;16:39–54. doi:10.2147/tcrm.S232033
16. FitzGerald JD, Dalbeth N, Mikuls T, et al. 2020 American College of Rheumatology Guideline for the Management of Gout. *Arthritis Care Res*. 2020;72(6):744–760. doi:10.1002/acr.24180
17. Stamp LK, Barclay ML. How to prevent allopurinol hypersensitivity reactions? *Rheumatology*. 2018;57(suppl_1):i35–i41. doi:10.1093/rheumatology/kex422
18. Hoyer D, Atti C, Nuding S, Vogt A, Sedding DG, Schott A. Toxic Epidermal Necrolysis Caused by Allopurinol: a Serious but Still Underestimated Adverse Reaction. *Am J Case Rep*. 2021;22:e932921. doi:10.12659/ajcr.932921
19. Jordan A, Gresser U. Side Effects and Interactions of the Xanthine Oxidase Inhibitor Febuxostat. *Pharmaceuticals*. 2018;11(2):51. doi:10.3390/ph11020051
20. Strilchuk L, Fogacci F, Cicero AF. Safety and tolerability of available urate-lowering drugs: a critical review. *Expert Opin Drug Saf*. 2019;18(4):261–271. doi:10.1080/14740338.2019.1594771
21. Chang YH, Chiang YF, Chen HY, et al. Anti-Inflammatory and Anti-Hyperuricemic Effects of Chrysin on a High Fructose Corn Syrup-Induced Hyperuricemia Rat Model via the Amelioration of Urate Transporters and Inhibition of NLRP3 Inflammasome Signaling Pathway. *Antioxidants*. 2021;10:4. doi:10.3390/antiox10040564
22. Chen Y, Li C, Duan S, Yuan X, Liang J, Hou S. Curcumin attenuates potassium oxonate-induced hyperuricemia and kidney inflammation in mice. *Biomed Pharmacother*. 2019;118:109195. doi:10.1016/j.biopha.2019.109195
23. Zhang D, Zhao M, Li Y, Zhang D, Yang Y, Li L. Natural Xanthine Oxidase Inhibitor 5-O-Caffeoylshikimic Acid Ameliorates Kidney Injury Caused by Hyperuricemia in Mice. *Molecules*. 2021;26:23. doi:10.3390/molecules26237307
24. Wang R, Ma CH, Zhou F, Kong LD. Siwu decoction attenuates oxonate-induced hyperuricemia and kidney inflammation in mice. *Chin J Nat Med*. 2016;14(7):499–507. doi:10.1016/s1875-5364(16)
25. He L, Rong X, Jiang JM, Liu PQ, Li Y. Amelioration of anti-cancer agent Adriamycin-induced nephrotic syndrome in rats by Wulingsan (Gorei-San), a blended traditional Chinese herbal medicine. *Food Chem Toxicol*. 2008;46(5):1452–1460. doi:10.1016/j.fct.2007.12.005
26. Yang Y, Zhang DM, Liu JH, et al. Wuling San protects kidney dysfunction by inhibiting renal TLR4/MyD88 signaling and NLRP3 inflammasome activation in high fructose-induced hyperuricemic mice. *J Ethnopharmacol*. 2015;169:49–59. doi:10.1016/j.jep.2015.04.011
27. Ding XQ, Pan Y, Wang X, Ma YX, Kong LD. Wuling san ameliorates urate under-excretion and renal dysfunction in hyperuricemic mice. *Chin J Nat Med*. 2013;11(3):214–221. doi:10.1016/s1875-5364(13)
28. Oh YC, Jeong YH, Ha JH, Cho WK, Ma JY. Oryeongsan inhibits LPS-induced production of inflammatory mediators via blockade of the NF-kappaB, MAPK pathways and leads to HO-1 induction in macrophage cells. *BMC Complement Altern Med*. 2014;14:242. doi:10.1186/1472-6882-14-242
29. Yang M, Chen JL, Xu LW, Ji G. Navigating traditional Chinese medicine network pharmacology and computational tools. *Evid Based Complement Alternat Med*. 2013;2013:731969. doi:10.1155/2013/731969
30. Li S, Fan TP, Jia W, Lu A, Zhang W. Network pharmacology in traditional Chinese medicine. *Evid Based Complement Alternat Med*. 2014;2014:138460. doi:10.1155/2014/138460
31. Ru J, Li P, Wang J, et al. TCMSP: a database of systems pharmacology for drug discovery from herbal medicines. *J Cheminform*. 2014;6:13. doi:10.1186/1758-2946-6-13
32. Wu Y, Zhang F, Yang K, et al. SymMap: an integrative database of traditional Chinese medicine enhanced by symptom mapping. *Nucleic Acids Res*. 2019;47(D1):D1110–D1117. doi:10.1093/nar/gky1021
33. Kim S, Thiessen PA, Bolton EE, et al. PubChem Substance and Compound databases. *Nucleic Acids Res*. 2016;44(D1):D1202–D1213. doi:10.1093/nar/gkv951
34. Gfeller D, Grosdidier A, Wirth M, Daina A, Michielin O, Zoete V. SwissTargetPrediction: a web server for target prediction of bioactive small molecules. *Nucleic Acids Res*. 2014;42(WebServer issue):W32–38. doi:10.1093/nar/gku293
35. Amberger JS, Bocchini CA, Schiettecatte F, Scott AF, Hamosh A. OMIM.org: online Mendelian Inheritance in Man (OMIM®), an online catalog of human genes and genetic disorders. *Nucleic Acids Res*. 2015;43:D789–798. doi:10.1093/nar/gku1205
36. Wang Y, Zhang S, Li F, et al. Therapeutic target database enriched resource for facilitating research and early development of targeted therapeutics. *Nucleic Acids Res*. 2020;48(D1):D1031–D1041. doi:10.1093/nar/gkz981
37. Piñero J, Ramirez-Anguita JM, Saüch-Pitarch J, et al. The DisGeNET knowledge platform for disease genomics: 2019 update. *Nucleic Acids Res*. 2020;48(D1):D845–D855. doi:10.1093/nar/gkz1021
38. Safran M, Dalah I, Alexander J, et al. GeneCards Version 3: the human gene integrator. *Database*. 2010;2010:baq020. doi:10.1093/database/baq020
39. Wishart DS, Feunang YD, Guo AC, et al. DrugBank 5.0: a major update to the DrugBank database for 2018. *Nucleic Acids Res*. 2018;46(D1):D1074–D1082. doi:10.1093/nar/gkx1037
40. Szklarczyk D, Gable AL, Nastou KC, et al. The STRING database in 2021: customizable protein-protein networks, and functional characterization of user-uploaded gene/measurement sets. *Nucleic Acids Res*. 2021;49(D1):D605–D612. doi:10.1093/nar/gkaa1074
41. Sussman JL, Lin D, Jiang J, et al. Protein Data Bank (PDB): database of three-dimensional structural information of biological macromolecules. *Acta Crystallogr D Biol Crystallogr*. 1998;54(Pt 1):1078–1084. doi:10.1107/s0907444998009378
42. Han J, Wang X, Hou J, Liu Y, Liu P, Zhao T. Using Network Pharmacology to Explore the Mechanism of Peach Kernel-Safflower in the Treatment of Diabetic Nephropathy. *Biomed Res Int*. 2021;2021:6642584. doi:10.1155/2021/6642584
43. Cao X, Liang Y, Liu R, et al. Uncovering the Pharmacological Mechanisms of Gexia-Zhuyu Formula (GXZY) in Treating Liver Cirrhosis by an Integrative Pharmacology Strategy. *Front Pharmacol*. 2022;13:793888. doi:10.3389/fphar.2022.793888
44. Zhang M, Zhu X, Wu J, et al. Prevalence of Hyperuricemia Among Chinese Adults: findings From Two Nationally Representative Cross-Sectional Surveys in 2015–16 and 2018–19. *Front Immunol*. 2021;12:791983. doi:10.3389/fimmu.2021.791983

45. Pathmanathan K, Robinson PC, Hill CL, Keen HI. The prevalence of gout and hyperuricaemia in Australia: an updated systematic review. *Semin Arthritis Rheum.* 2021;51(1):121–128. doi:10.1016/j.semarthrit.2020.12.001
46. Chen-Xu M, Yokose C, Rai SK, Pillinger MH, Choi HK. Contemporary Prevalence of Gout and Hyperuricemia in the United States and Decadal Trends: the National Health and Nutrition Examination Survey, 2007–2016. *Arthritis Rheumatol.* 2019;71(6):991–999. doi:10.1002/art.40807
47. Soskind R, Abazia DT, Bridgeman MB. Updates on the treatment of gout, including a review of updated treatment guidelines and use of small molecule therapies for difficult-to-treat gout and gout flares. *Expert Opin Pharmacother.* 2017;18(11):1115–1125. doi:10.1080/14656566.2017.1349099
48. Benn CL, Dua P, Gurrell R, et al. Physiology of Hyperuricemia and Urate-Lowering Treatments. *Front Med.* 2018;5:160. doi:10.3389/fmed.2018.00160
49. Lin E, Ho L, Lin MS, Huang MH, Chen WC. Wu-Ling-San formula prophylaxis against recurrent calcium oxalate nephrolithiasis - a prospective randomized controlled trial. *Afr J Tradit Complement Altern Med.* 2013;10(5):199–209. doi:10.4314/ajtcam.v10i5.1
50. Chen YC, Ho CY, Chen LD, Hsu SF, Chen WC. Wu-Ling-San formula inhibits the crystallization of calcium oxalate in vitro. *Am J Chin Med.* 2007;35(3):533–541. doi:10.1142/s0192415x07005041
51. Alam MB, Chowdhury NS, Sohrab MH, Rana MS, Hasan CM, Lee SH. Cerevisterol Alleviates Inflammation via Suppression of MAPK/NF- κ B/AP-1 and Activation of the Nrf2/HO-1 Signaling Cascade. *Biomolecules.* 2020;10(2):199. doi:10.3390/biom10020199
52. Lodhi S, Vadnere GP, Patil KD, Patil TP. Protective effects of luteolin on injury induced inflammation through reduction of tissue uric acid and pro-inflammatory cytokines in rats. *J Tradit Complement Med.* 2020;10(1):60–69. doi:10.1016/j.jtcme.2019.02.004
53. Alekhya Sita GJ, Gowthami M, Srikanth G, et al. Protective role of luteolin against bisphenol A-induced renal toxicity through suppressing oxidative stress, inflammation, and upregulating Nrf2/ARE/ HO-1 pathway. *IUBMB Life.* 2019;71(7):1041–1047. doi:10.1002/iub.2066
54. Kobori M, Yoshida M, Ohnishi-Kameyama M, Shinmoto H. Ergosterol peroxide from an edible mushroom suppresses inflammatory responses in RAW264.7 macrophages and growth of HT29 colon adenocarcinoma cells. *Br J Pharmacol.* 2007;150(2):209–219. doi:10.1038/sj.bjp.0706972
55. Duan C, Ge X, Wang J, Wei Z, Feng WH, Wang J. Ergosterol peroxide exhibits antiviral and immunomodulatory abilities against porcine deltacoronavirus (PDCoV) via suppression of NF- κ B and p38/MAPK signaling pathways in vitro. *Int Immunopharmacol.* 2021;93:107317. doi:10.1016/j.intimp.2020.107317
56. de Souza MR, de Paula CA, Pereira de Resende ML, Grabe-Guimarães A, de Souza Filho JD, Saúde-Guimarães DA. Pharmacological basis for use of *Lychnophora trichocarpa* in gouty arthritis: anti-hyperuricemic and anti-inflammatory effects of its extract, fraction and constituents. *J Ethnopharmacol.* 2012;142(3):845–850. doi:10.1016/j.jep.2012.06.012
57. Kaul S, Gupta M, Bandyopadhyay D, et al. Gout Pharmacotherapy in Cardiovascular Diseases: a Review of Utility and Outcomes. *Am J Cardiovasc Drugs.* 2021;21(5):499–512. doi:10.1007/s40256-020-00459-1
58. Zhang S, Wang Y, Cheng J, et al. Hyperuricemia and Cardiovascular Disease. *Curr Pharm Des.* 2019;25(6):700–709. doi:10.2174/1381612825666190408122557
59. Zhou Y, Zhao M, Pu Z, Xu G, Li X. Relationship between oxidative stress and inflammation in hyperuricemia: analysis based on asymptomatic young patients with primary hyperuricemia. *Medicine.* 2018;97(49):e13108. doi:10.1097/md.00000000000013108
60. Estevez-Garcia IO, Gallegos-Nava S, Vera-Pérez E, et al. Levels of Cytokines and MicroRNAs in Individuals With Asymptomatic Hyperuricemia and Ultrasonographic Findings of Gout: a Bench-to-Bedside Approach. *Arthritis Care Res.* 2018;70(12):1814–1821. doi:10.1002/acr.23549
61. Luis-Rodríguez D, Donate-Correa J, Martín-Núñez E, et al. Serum urate is related to subclinical inflammation in asymptomatic hyperuricaemia. *Rheumatology.* 2021;60(1):371–379. doi:10.1093/rheumatology/keaa425
62. Martínez-Reyes CP, Manjarrez-Reyna AN, Méndez-García LA, et al. Uric Acid Has Direct Proinflammatory Effects on Human Macrophages by Increasing Proinflammatory Mediators and Bacterial Phagocytosis Probably via URAT1. *Biomolecules.* 2020;10(4):576. doi:10.3390/biom10040576
63. Yokose K, Sato S, Asano T, et al. TNF- α potentiates uric acid-induced interleukin-1 β (IL-1 β) secretion in human neutrophils. *Mod Rheumatol.* 2018;28(3):513–517. doi:10.1080/14397595.2017.1369924
64. Temmoku J, Fujita Y, Matsuoka N, et al. Uric acid-mediated inflammasome activation in IL-6 primed innate immune cells is regulated by baricitinib. *Mod Rheumatol.* 2021;31(1):270–275. doi:10.1080/14397595.2020.1740410
65. Li D, Wang L, Ou J, et al. Reactive oxygen species induced by uric acid promote NRK-52E cell apoptosis through the NEK7-NLRP3 signaling pathway. *Mol Med Rep.* 2021;24(4):548. doi:10.3892/mmr.2021.12368
66. Nie Q, Liu M, Zhang Z, Zhang X, Wang C, Song G. The effects of hyperuricemia on endothelial cells are mediated via GLUT9 and the JAK2/STAT3 pathway. *Mol Biol Rep.* 2021;48(12):8023–8032. doi:10.1007/s11033-021-06840-w
67. Zhang Y, Tan X, Lin Z, et al. Fucoic acid from *Laminaria japonica* Inhibits Expression of GLUT9 and URAT1 via PI3K/Akt, JNK and NF- κ B Pathways in Uric Acid-Exposed HK-2 Cells. *Mar Drugs.* 2021;19(5):3256. doi:10.3390/md19050238
68. Oberbach A, Neuhaus J, Jehmlich N, et al. A global proteome approach in uric acid stimulated human aortic endothelial cells revealed regulation of multiple major cellular pathways. *Int J Cardiol.* 2014;176(3):746–752. doi:10.1016/j.ijcard.2014.07.102
69. Wang G, Zuo T, Li R. The mechanism of Arhalofenate in alleviating hyperuricemia-Activating PPAR γ thereby reducing caspase-1 activity. *Drug Dev Res.* 2020;81(7):859–866. doi:10.1002/ddr.21699
70. Wang X, Deng J, Xiong C, et al. Treatment with a PPAR- γ Agonist Protects Against Hyperuricemic Nephropathy in a Rat Model. *Drug Des Devel Ther.* 2020;14:2221–2233. doi:10.2147/dddt.S247091

Drug Design, Development and Therapy

Dovepress

Publish your work in this journal

Drug Design, Development and Therapy is an international, peer-reviewed open-access journal that spans the spectrum of drug design and development through to clinical applications. Clinical outcomes, patient safety, and programs for the development and effective, safe, and sustained use of medicines are a feature of the journal, which has also been accepted for indexing on PubMed Central. The manuscript management system is completely online and includes a very quick and fair peer-review system, which is all easy to use. Visit <http://www.dovepress.com/testimonials.php> to read real quotes from published authors.

Submit your manuscript here: <https://www.dovepress.com/drug-design-development-and-therapy-journal>